Available online at www.sciencedirect.com
SCIENCE DIRECT
Journal of Photochemistry and Photobiology A: Chemistry 177 (2006) 164–169
Journal of Photochemistry and Photobiology A:Chemistry
www.elsevier.com/locate/jphotochem

Photo-physical behavior as chemosensor properties of anthracene-anchored 1,3-di-derivatives of lower rim calix[4]arene towards divalent transition metal ions

Ajeet Kumar, Amjad Ali, Chebrolu P. Rao *

Bioinorganic Laboratory, Department of Chemistry, Indian Institute of Technology Bombay, Mumbai 400076, India

Received 30 March 2005; accepted 16 May 2005
Available online 24 June 2005

Abstract

Anthracene anchored 1,3-di-derivatives of lower rim *p-tert*-butyl-calix[4]arene were synthesized and characterized. These derivatives were subjected to the binding studies with the divalent metal ions, viz., Mg^{2+}, Mn^{2+}, Fe^{2+}, Co^{2+}, Ni^{2+}, Cu^{2+} and Zn^{2+} using fluorescence and absorption spectra. The imine moiety that is in conjugation with the anthryl unit is responsible for quenching the fluorescence in the absence of metal ion, however, in the presence of Fe^{2+} and Cu^{2+}, the spectra showed very high enhancement in fluorescence intensity indicating that the lone pair present on the imine-N is involved in the metal ion binding and as a result the photo-induced electron transfer is prevented. Based on the photo-physical studies, it has been found that the anthracene derivative that is coupled with the calix[4]arene unit through an imine bond acts as a chemosensor for Fe^{2+} and Cu^{2+}. The fluorescence studies are further augmented by the absorption spectra.

Keywords: *p-tert*-Butyl-calix[4]arene; Anthracene-imine derivative; Fluorescence enhancement; Photo-induced electron transfer; Chemosensor

1. Introduction

Calixarenes are ubiquitous containing both hydrophobic and hydrophilic compartments together in the same molecule. Organic synthesis ensures building-up of coordination cores either on the lower rim or on the upper rim and hence the resulting derivatives are good biomimetic models [1,2]. In this context binding and/or recognition of organic or inorganic moieties is of utmost importance. In order to evaluate such properties of these derivatives, sensitive techniques that are easy to monitor are essential. In this regard, fluorescence spectroscopy offers an efficient and convenient way. Hence the calixarene derivatives with appropriate binding cores and yet possessing fluorescent probe are of great advantage. Recent literature witnessed the binding of alkali and alkaline earth ions with the lower rim calix[4]arene derivatives possessing fluorophores where high mole ratios of metal ion to the ligand were used to get significant changes in the fluorescence [3–7]. On the other hand, there are only few reports of such studies regarding the binding of transition metal ions to fluorophore bound calix[4]arene derivatives [8,9]. Therefore, this paper demonstrates the differential interaction of various metal ions with lower rim based di-derivatives possessing anthryl moiety using their fluorescence-on/off behavior besides providing their synthesis and characterization.

2. Experimental

2.1. Materials

9-Anthraldehyde, anthracene, 9-chloromethylanthracene and the metal perchlorates (caution: perchlorate salts are expected to be handled with appropriate care) were purchased from Sigma–Aldrich Chem. Co. Analytical grade solvents obtained locally were purified and dried by routine procedures immediately before use.

* Corresponding author. Fax: +91 22 2572 3480.
E-mail address: cprao@chem.iitb.ac.in (C.P. Rao).

1010-6030/$ – see front matter © 2005 Elsevier B.V. All rights reserved.
doi:10.1016/j.jphotochem.2005.05.021

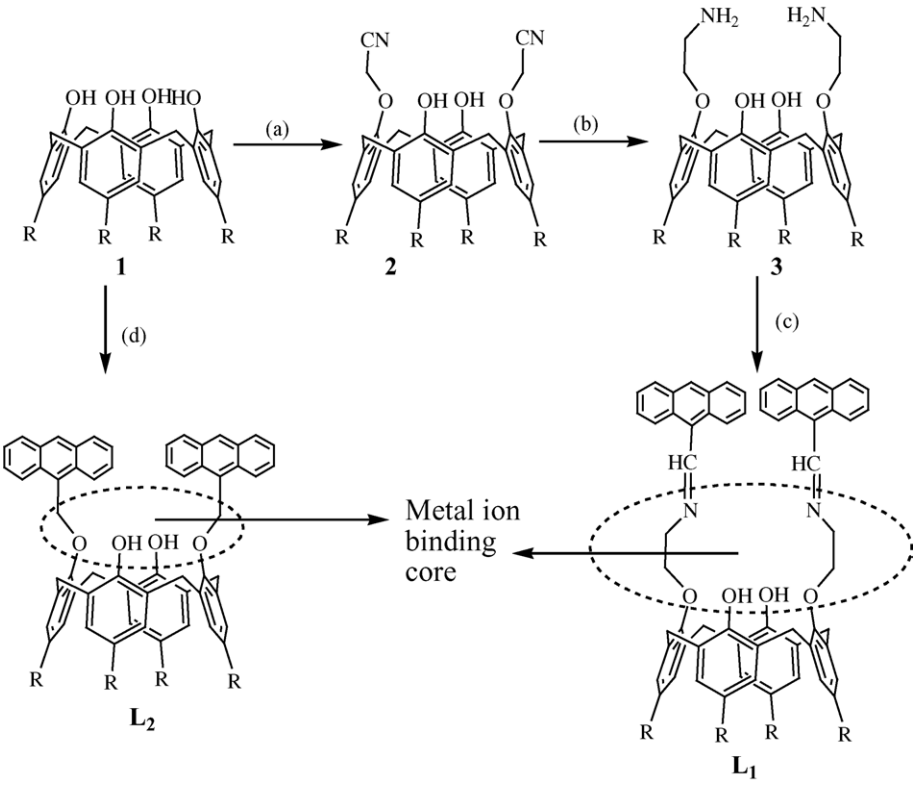

Scheme 1. Synthesis of L_1 and L_2: (a) **1** (1.0 g, 1.55 mmol), K_2CO_3 (1.0 g, 7.25 mmol), bromoacetonitrile (0.8 g, 8.31 mmol), 50 mL CH_3CN, reflux under N_2 for 7 h; (b) **2** (4.70 g, 6.50 mmol), $LiAlH_4$ (2.0 g, 5.1 mmol), 250 mL $C_2H_5OC_2H_5$, reflux for 5 h; (c) **3** (100 mg, 0.136 mmol), 9-anthraldehyde (56.0 mg, 0.272 mmol), 10 mL EtOH, pH range is maintained between 5 and 6 by adding appropriate amount of H_2SO_4, reflux for 3 h; (d) **1** (0.5 g, 0.675 mmol), 9-chloromethylanthracene (0.45 g, 2.02 mmol), K_2CO_3 (0.745 g, 5.40 mmol) 25 mL CH_3CN. R = *tert*-butyl.

2.2. Synthesis of lower rim calix[4]arene fluorophores

Reaction of bromoacetonitrile with *p-tert*-butyl-calix[4] arene, **1** results in the di-nitrile derivative **2** which upon reduction by $LiAlH_4$ yields the di-amine derivative **3**. This di-amine derivative **3** results in the formation of L_1 when reacted with 9-anthraldehyde [10,11]. On the other hand, reaction of **1** with 9-chloromethylanthracene directly results in the formation of L_2. All these steps are shown in Scheme 1 and all the products were characterized [12–16].

2.3. UV–vis and fluorescence studies

The ligands are dissolved in $CHCl_3$ and the metal perchlorates in MeOH, and all the bulk solutions are made to 0.001 M concentration. All the measurements have been made in 1 cm quartz cells and maintained a final ligand concentration of 10 μM and the concentration of metal perchlorates were varied accordingly in order to result in requisite mole ratios of metal ion to the ligand. During the titration of the ligand with metal perchlorates, the total volume of the solution is maintained constant (3 mL) in each case by adding appropriate volume of 5% MeOH–$CHCl_3$.

Fluorescence spectra were measured on Perkin-Elmer LS55 by exciting at 340 nm and absorption spectra of the same solutions were measured on Shimadzu UV-2101PC in the range 320–500 nm. Normalized emission intensities (I/I_0) are plotted against the mole ratio of metal ion to the ligand. The binding constants of the complexes formed in the solution have been quantitatively estimated by plotting $\log[(I - I_0)/(I^* - I)]$ versus log[S] (I_0, intensity with no metal ion; I^*, maximum Intensity; I, intensity in the presence of various ratios of metal salt; and S, concentration of the metal salt added). The slope of the straight line gives the ratio of the ligand versus metal cation in the fully saturated case and pK_{ass} for the complex equals to the value of log[S] at $\log[(I - I_0)/(I^* - I)] = 0$. The quantum yields of the ligand L_1 and the complexes were measured with respect to anthracene ($\varphi = 0.27 \pm 0.03$ in EtOH).

3. Results and discussion

L_1, L_2 and all the intermediate products in the synthesis were well characterized [12–16]. Proton NMR data (two doublets for methylene bridged protons with $J = 13$ Hz) is consistent with the presence of 1,3-di-derivatives being in their cone conformation in case of L_1 as well as in L_2. The ligand L_1 has two imine bonds in conjugation with anthracene unit, two phenolic–OH groups and two ether oxygens of the

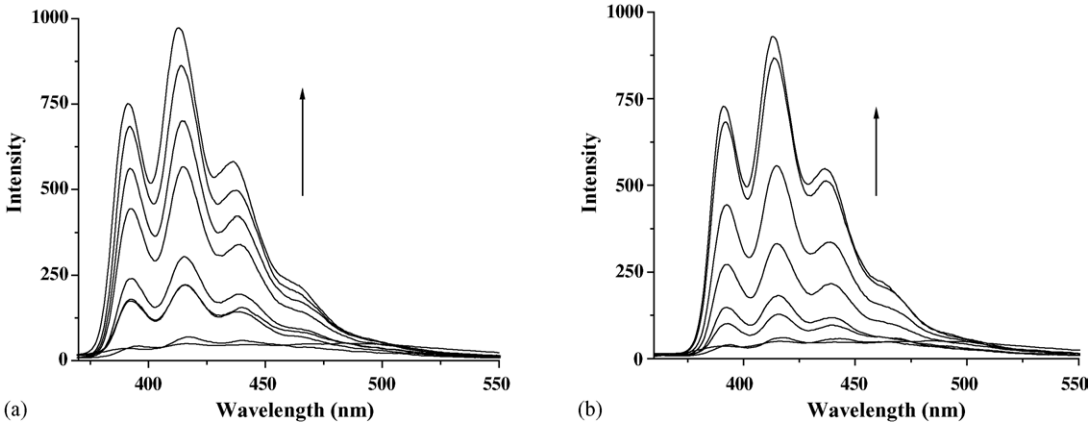

Fig. 1. Fluorescence spectra of L_1 as a function of added metal ion concentration (varying L_1/M^{2+} ratios): (a) Fe^{2+} (1:1–1:60); (b) Cu^{2+} (1:1–1:50).

pendant present on the lower rim and these provide potential sites for metal ion binding (Scheme 1). The binding strength of these groups is expected to differ depending upon the nature of the metal ion and thus the interaction of the metal ion would influence the fluorescence emission to different extents owing to its coordination preferences. Single crystal X-ray analysis of other 1,3-di-derivatives possessing amide pendants indicated that there exists hydrogen bond interaction between the phenolic–OH and the ether oxygen of the adjacent pendant resulting in narrowing of the entry for species towards the lower rim [17].

3.1. Emission and absorption studies

3.1.1. In the absence of metal ion

Free L_1 shows very weak anthracene-type emission from locally excited lowest ($\pi \rightarrow \pi^*$) state in $CHCl_3$/MeOH (19:1) at room temperature as compared to the simple anthracene due to quenching by a conjugated imine moiety (lone pair of electrons on nitrogen) and the quenching is at least by ~35-fold. This imine group, as a spacer, makes the system rigid and the lone pair is delocalized on to the π-cloud of the anthracene unit. Such rigidity provides a favorable orbital overlap between imine-N and the π-orbital of anthracene, and hence results in photoinduced electron transfer (PET) [18]. On the other hand, L_2 having no interconnecting imine group between the anthracene and calixarene portions (Scheme 1) exhibits an emission that is quite similar to that of the anthracene it self, but with only a 3.5 fold quenching, i.e., 10 times lower than the L_1.

3.1.2. In the presence of metal ions

Effect of metal ions, viz., Mg^{2+}, Mn^{2+}, Fe^{2+}, Co^{2+}, Ni^{2+}, Cu^{2+} and Zn^{2+} on L_1 were studied using fluorescence and absorption spectra in $CHCl_3$/MeOH (19:1). Fluorescence intensity of L_1 enhances as a function of the addition of Fe^{2+} and Cu^{2+} dramatically as shown in Fig. 1. Either in the emission spectra (Fig. 2a) or in the absorption spectra (Fig. 2b), when L_1 is bound to Fe^{2+} and Cu^{2+}, it exhibits a spectrum having features very similar to the original anthracene spectrum itself. All this indicates the role of the lone pair on the imine-N in quenching the fluorescence in the free ligand and

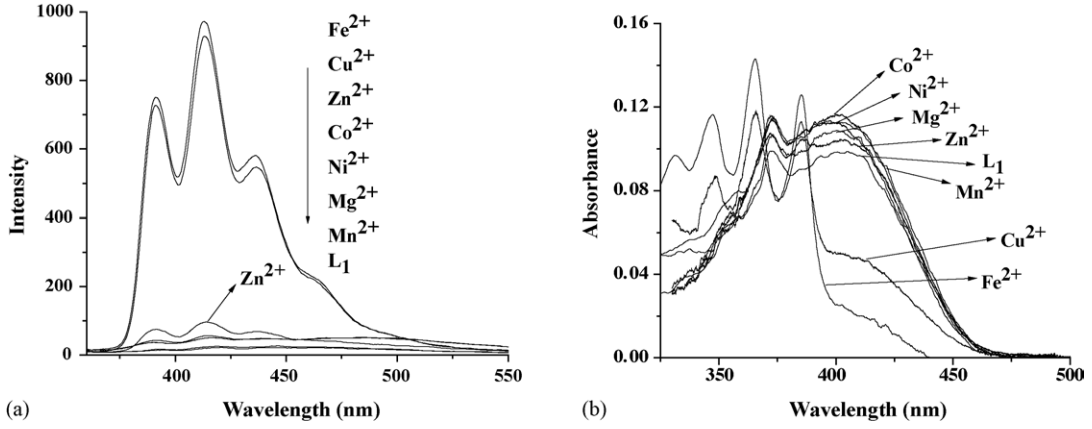

Fig. 2. Spectral traces at L_1/M^{2+} ratio being 1:50: (a) fluorescence spectra (excitation wavelength of 340 nm); (b) absorption spectra.

Table 1
Quantum yield (φ) of L_1 and its metal ion complexes

$L_1 + M^{2+}$	φ
L_1	0.0036
Fe^{2+}	0.061
Cu^{2+}	0.056
Zn^{2+}	0.0107
Co^{2+}	0.0064
Mn^{2+}	0.0061
Ni^{2+}	0.0060
Mg^{2+}	0.0054

the reversal of this quenching by the metal ion binding that utilizes the lone pair. The increase in the fluorescence intensity of L_1 follow a trend, $Fe^{2+} \sim Cu^{2+} >> Zn^{2+}$, where as the remaining metal ions, viz., Mg^{2+}, Mn^{2+}, Co^{2+}, Ni^{2+} shows no considerable effect. Fluorescence quantum yields of L_1 in the presence of different metal ions measured relative to the anthracene are shown in Table 1. In presence of Fe^{2+} and Cu^{2+} the quantum yield enhances by ~15 times.

The normalized intensity for Cu^{2+} and Fe^{2+} are plotted against the metal to the ligand mole ratio as shown in Fig. 3 and the curves indicate that while the binding of Fe^{2+} is a three step process (Fig. 3a), that of the Cu^{2+} (Fig. 3b) and Zn^{2+} (Fig. 3c) are two step processes. These binding steps with L_1 are attributable to different binding modes present in the ligand L_1 as shown in Scheme 2. Owing to the HSAB principle, the divalent transition metal ions are expected to have higher affinity towards imine over that of the oxygen ligating centers. Hence, the first step of binding of these metal ions with L_1 is at the imine functions and the second step arises from the binding of two ether oxygens of the pendants. The third step in the Fe^{2+} curve can be explained owing to the binding of the two phenolic–OH groups with the metal ion center. As a function of step-wise binding, there occur concomitant changes in the geometry around the metal ion that enters the binding core as well as in the geometry of the fluorescing group. Binding of transition metal ion at the imine center quenches the effect of lone pair present on nitrogen that is responsible for the conjugation and thereby enhances the intensity of fluorescence. At any given $[M^{2+}/L_1]$ ratio, the fluorescence enhancement is ~5.5-fold for Fe^{2+}/Zn^{2+} or Cu^{2+}/Zn^{2+}. The association constants ($\log K_{ass}$), for the corresponding steps were estimated using $\log[(I - I_0)/(I^* - I)]$ versus log[S], to be 4.80, 3.80, 3.39 for Fe^{2+}, 4.54, 3.68 for Cu^{2+}, and 4.74, 3.74 for Zn^{2+} towards L_1. Analysis of these plots by equilibrium shift method yields 1:1 complex [6]. While the number of steps observed could be used to differentiate the Fe^{2+} from that of Cu^{2+}, the fluorescence enhancement ratio can be used to differentiate Zn^{2+} from these ions. Thus, L_1 can act as fluorescence-on chemosensor towards these ions. This is further supported by the fact that the enhancement in I/I_0 is higher by at least 10 times for L_1 (Fig. 3a and b) when compared to a control ligand, L_2 (Fig. 4) where there is no imine group involved, either for Fe^{2+} or for Cu^{2+}. Similar study carried out with an upper rim-based fluorophore [18] on the other hand exhibited large changes in fluorescence intensity only with Co^{3+} and Cu^{2+}. However, their studies were not augmented by a corresponding calixarene control ligand.

As evident from the literature, calix[4]arene lower rim derivatives bearing fluorophore sensors showed measurable changes in fluorescence intensity or in absorption intensity

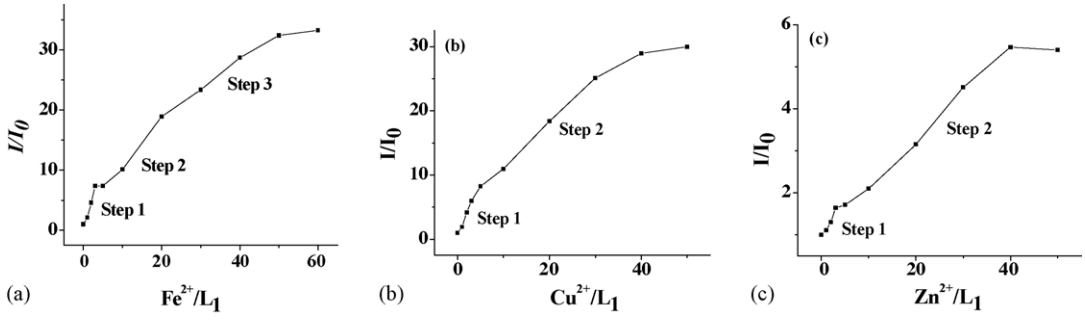

Fig. 3. Plots of metal ion to the ligand mole ratio (M^{2+}/L_1) vs. normalized intensity (I/I_0). Step-wise binding is designated on the graph and for the details of the steps, Scheme 2 be referred.

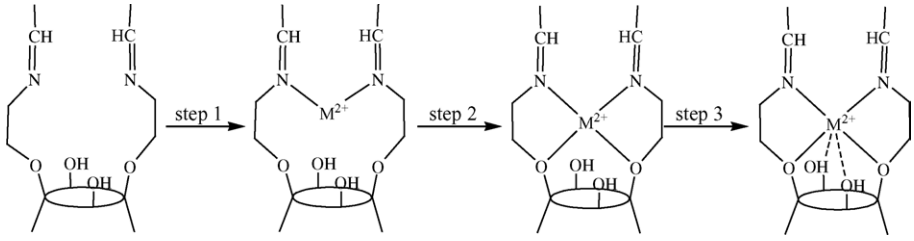

Scheme 2. Step-wise binding of M^{2+} (Fe^{2+}, Cu^{2+} or Zn^{2+}) ion by the ligating centers present in the binding core of L_1. Step 3 is valid only in case of Fe^{2+}.

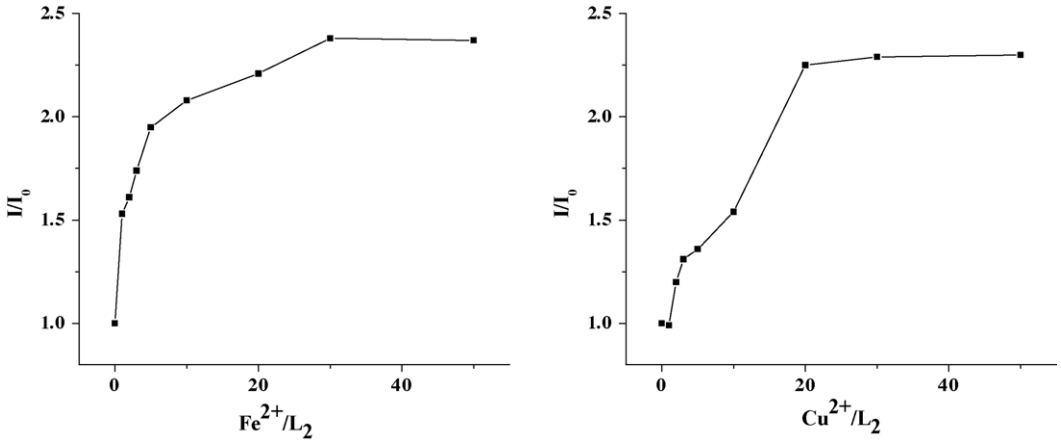

Fig. 4. Plots of metal ion to the ligand mole ratio (M^{2+}/L_2) vs. normalized intensity (I/I_0).

only at high metal ion to the ligand ratios [3–9]. Indeed this ratio is very high in case of alkali and alkaline earth ion sensors as reported in the literature.

4. Conclusions

Presence of the conjugated imine moiety in L_1 is responsible for the fluorescence quenching of the anthryl unit owing to the photo-induced electron transfer from the imine-N to the anthryl π cloud. Binding of Fe^{2+} and Cu^{2+} with the imine-N prevents the electron transfer from this group to the photo-excited anthryl unit. Clearly the fluorescence enhancement of L_1 in presence of Fe^{2+} and Cu^{2+} is much higher than that observed for L_2 in presence of the same metal ions. Depending upon the metal ion to the ligand ratio, the fluorescence enhancement in L_1 is 10–14-fold high as compared to L_2. This can be attributed to the involvement of the lone pair on nitrogen of the imine moiety in L_1 with the metal ion binding. Thus, the calix[4]arene derivative containing the imine group, viz., L_1 is more efficient and hence can be a better chemosensor towards transition metal ions, particularly the Fe^{2+} and Cu^{2+}, as compared to L_2, its counter part having no imine moiety. This deduction is in agreement with the fact that the transition metal ions have greater affinity towards imine moiety. In case of Fe^{2+} and Cu^{2+}, the absorption spectra also exhibited vivid changes in the region 325–500 nm, owing to the strong and specific binding of these two metal ions to L_1 over the other ions reported in this paper. Thus, L_1, a calix[4]arene lower rim fluorophore is a potential chemosensor for Fe^{2+} and Cu^{2+}.

Acknowledgements

C.P.R. acknowledges the financial support from the CSIR and DST, New Delhi, and IIT Bombay for fluorescence facility at the Department of Chemistry. A.A. acknowledges the SRF fellowship from CSIR.

References

[1] C.D. Gutsche, in: J.F. Stoddart (Ed.), Calixarenes Revisited, Monographs in Supramolecular Chemistry, Royal Society of Chemistry, Cambridge, 1998.
[2] L. Mandolini, R. Ungaro (Eds.), Calixarenes in Action, Imperial College Press, London, 2000.
[3] J.S. Kim, O.J. Shon, J.K. Lee, S.H. Lee, J.Y. Kim, K.-M. Park, S.S. Lee, J. Org. Chem. 67 (2002) 1372.
[4] J.S. Kim, O.J. Shon, J.A. Rim, S.K. Kim, J. Yoon, J. Org. Chem. 67 (2002) 2348.
[5] H. Matsumoto, S. Shinkai, Tet. Lett. 37 (1996) 77.
[6] I. Aoki, T. Sakaki, S. Shinkai, J. Chem. Soc. Chem. Commun. (1992) 730.
[7] I. Aoki, H. Kawabata, K. Nakashima, S. Shinkai, J. Chem. Soc. Chem. Commun. (1991) 1717.
[8] F. Unob, Z. Asfari, J. Vicens, Tet. Lett. 39 (1998) 2951.
[9] Y.-D. Cao, Q.-Y. Zheng, C.-F. Chen, Z.-T. Huang, Tet. Lett. 44 (2003) 4751.
[10] W.-C. Zhang, Z.-T. Huang, Synthesis (1997) 1073.
[11] F. Szemes, D. Hesek, Z. Chen, S.W. Dent, M.G.B. Drew, A.J. Goulden, A.R. Graydon, A. Grieve, R.J. Mortimer, T. Wear, J.S. Weightman, P.D. Beer, Inorg. Chem. 35 (1996) 5868.
[12] **1**: Yield 48%. FTIR (KBr matrix, cm^{-1}): 3186 (ν_{OH}); 1206 (ν_{C-O}). ^1H NMR ($CDCl_3$, δ ppm): 10.33 (s, 4H, Ar─*OH*); 7.05 (s, 8H, Ar─*H*); 4.30 (br, 4H, Ar─C*H*$_2$─Ar); 3.50 (br, 4H, Ar─C*H*$_2$─Ar); 1.26 (s, 36H, C(C*H*$_3$)$_3$); Anal. calcd.(%) for $C_{51}H_{64}O_4$: Calc. C, 82.7; H, 8.64; found C, 82.61; H, 8.61.
[13] **2**: Yield 80%; FTIR (KBr disc) (cm^{-1}) 1482 (ν_{CN}), 3515 (ν_{OH}); ^1H NMR ($CDCl_3$, δ ppm): 7.119 (s, 4H, Ar─*H*); 6.727 (s, 4H, Ar─*H*); 4.808 (s, 4H, OC*H*$_2$); 4.221 (d, 4H, Ar─C*H*$_2$─Ar, *J* = 13.55 Hz); 3.447 (d, 4H, Ar─C*H*$_2$─Ar, *J* = 13.55 Hz); 1.324 (s, 18H, C(C*H*$_3$)$_3$); 0.880 (s, 18H, C(C*H*$_3$)$_3$); Anal.calcd (%) for $C_{48}H_{58}N_2O_4$: C, 79.33 H, 7.98; N, 3.86. Found: C, 78.49 H, 8.30; N, 3.92.
[14] **3**: Yield 85%; FTIR (KBr disc) (cm^{-1}) 3368 ($\nu_{OH/NH}$); m.p., 200 °C (decomposes); ^1H NMR ($CDCl_3$, δ ppm): 7.036 (s, 4H, Ar─*H*); 6.976 (s, 4H, Ar─*H*); 4.319 (d, 4H, Ar─C*H*$_2$─Ar, *J* = 12.82 Hz); 4.076 (t, 4H, OC*H*$_2$, *J* = 4.76, 4.76); 3.370 (d, 4H, Ar─C*H*$_2$─Ar, *J* = 12.82 Hz); 3.298 (t, NC*H*$_2$, *J* = 4.76, 4.76); 1.245 (s, 18H, C(C*H*$_3$)$_3$); 1.102 (s, 18H, C(C*H*$_3$)$_3$). FAB (+) MS: *m*/*z* 943 ($[M+H]^+$, 100%).
[15] **L$_1$**: Yield 30%; ^1H NMR ($CDCl_3$, δ ppm): 8.95 (s, *H*C═N, 2H); 8.35 (d, 4H, Anth-*H*, *J* = 8.6 Hz); 8.25 (s, 2H, Anth-*H*); 7.80 (d, 4H, Anth-*H*, *J* = 8.2 Hz); 7.32 (m, 8H, Anth-*H*); 7.23 (s, 2H, Ar─O*H*); 7.08 (s, 4H, Ar─*H*); 6.78 (s, 4H, Ar─*H*); 4.42 (d, 4H, Ar─C*H*$_2$─Ar, *J* = 13.1); 4.35 (t, 4H, OC*H*$_2$, *J* = 5.4, 5.5 Hz); 4.08

(t, 4H, Ar—CH_2—Ar, J = 5.1. 5.4 Hz); 3.35 (d, 4H, Ar—CH_2—Ar, J = 13.3Hz); 1.33 (s, 18H, C(CH_3)$_3$); 0.934 (s, 18H, C(CH_3)$_3$); FAB (+) MS: m/z 1112 ([M + H]$^+$, 35%): Anal.calcd (%) for $C_{78}H_{82}N_2O_4$.: C, 84.29 H, 7.44; N, 2.52. Found: C, 84.2 H, 7.22; N, 2.20.

[16] **L$_2$**: ^{1}H NMR ($CDCl_3$, δ ppm): 8.55 (s, 2H, Anth-*H*); 8.26 (d, 4H, Anth-*H*, J = 8.7); 8.01 (d, 4H, Anth-*H*, J = 8.4); 7.42 (s, 4H, Anth-*H*); 7.38 (s, 2H, Ar—O*H*); 6.85 (s, 4H, Ar-*H*); 6.75 (s, 4H, Ar); 6.15 (s, 4H, OCH_2); 4.10 (d, 4H, Ar—CH_2—Ar, J = 13.1Hz); 2.9 (d, 4H, Ar—CH_2—Ar, J = 13.3Hz); 1.22 (s, 18 H, C(CH_3)$_3$); 0.95 (s, 18H, C(CH_3)$_3$); FAB (+) MS: m/z 1028 ([M − H]$^+$, 25%); Anal.calcd (%) for $C_{74}H_{76}O_4$.: C, 86.34 H, 7.44. Found: C, 86.32 H, 7.52.

[17] P.V. Rao, C.P. Rao, E. Kolehmainen, E.K. Wegelius, K. Rissanen, Chem. Lett. (2001) 1176.

[18] H. Liu, B. Li, D. Liu, Z. Xu, Chem. Phys. Lett. 350 (2001) 441.